

# Sparse Spatial Smoothing: Reduced Complexity and Improved Beamforming Gain via Sparse Sub-Arrays

Yinyan Bu<sup>\*</sup>, Robin Rajamäki<sup>\*</sup>, Anand Dabak<sup>‡</sup>, Rajan Narasimha<sup>‡</sup>, Anil Mani<sup>‡</sup>, Piya Pal<sup>\*</sup>  
<sup>\*</sup>Department of Electrical and Computer Engineering, University of California San Diego, CA, USA

<sup>‡</sup>Texas Instruments, Dallas, TX, USA

**Abstract**—This paper addresses the problem of single snapshot Direction-of-Arrival (DOA) estimation, which is of great importance in a wide-range of applications including automotive radar. A popular approach to achieving high angular resolution when only one temporal snapshot is available is via subspace methods using spatial smoothing. This involves leveraging spatial shift-invariance in the antenna array geometry—typically a uniform linear array (ULA)—to rearrange the single snapshot measurement vector into a spatially smoothed matrix that reveals the signal subspace of interest. However, conventional approaches using spatially shifted ULA sub-arrays can lead to a prohibitively high computational complexity due to the large dimensions of the resulting spatially smoothed matrix. Hence, we propose to instead employ judiciously designed sparse sub-arrays, such as nested arrays, to reduce the computational complexity of spatial smoothing while retaining the aperture and identifiability of conventional ULA-based approaches. Interestingly, this idea also suggests a novel beamforming method which linearly combines multiple spatially smoothed matrices corresponding to different sets of shifts of the sparse (nested) sub-array. This so-called *shift-domain beamforming* method is demonstrated to boost the effective SNR, and thereby resolution, in a desired angular region of interest, enabling single snapshot low-complexity DOA estimation with identifiability guarantees.

**Index Terms**—Single-Snapshot DOA Estimation, Sparse Arrays, Spatial Smoothing, Shift-Domain Beamforming.

## I. INTRODUCTION

Direction-of-Arrival (DOA) estimation using multi-antenna arrays is essential in both wireless communications and radar. However, in many applications such as automotive radar [1] or joint communication and sensing [2], signal sources may be coherent due to multi-path and the environment highly dynamic due to the mobility of the sources or radar targets. As a result, the number of available temporal snapshots in a given coherence interval is limited; in the worst case, only single snapshot is available [1], [3]. In the single-snapshot scenario, a common practice is employing a uniform linear array (ULA), whose inherent shift-invariant structure can be leveraged to identify the DOAs from the signal subspace. In particular, spatial smoothing [4], [5] is typically used to reshape the single-snapshot measurement vector of the ULA into a structured matrix of appropriate rank, from which the DOAs can then be estimated using high-resolution subspace methods, such as MUSIC [6] or ESPRIT [7].

On the one hand, in some applications like automotive radar, the number of targets that need to be resolved in the angular

domain of any given range-Doppler bin can be small [8], therefore trading off identifiability for resolution is of great interest, where achieving superior resolution at the expense of identifiability may be acceptable. On the other hand, in addition to high angular resolution, many applications also require *fast* DOA estimation. For example, current automotive radars provide a whole radar cube—range, Doppler, and angle—every 50 ms [9]. Moreover, DOA estimation is typically implemented in embedded hardware with minimal computational resources. As the computational complexity of DOA estimation typically grows with the number of antennas, computational resources may become a limiting factor when deploying increasingly larger arrays—as is the trend at, for example, millimeter-wave wavelengths. For these reasons, low-complexity DOA estimation algorithms are needed.

In subspace methods, the main computational burden consists of computing the singular value decomposition (SVD) of the (possibly spatially smoothed) measurement matrix. However, in conventional spatial smoothing using ULA sub-arrays, the dimensions of this matrix are typically proportional to the number of antennas. Hence, the complexity of SVD may be prohibitively large in real-time applications employing many antennas. The number of antennas could be reduced by employing a sparse array geometry [10], which in addition to lowering hardware costs, can enhance resolution [11] and reduce mutual coupling [12]. However, compared to ULAs, which accommodate many choices of the sub-array used for spatial smoothing, designing sparse array geometries that are both amenable to spatial smoothing (by virtue of a shift-invariant structure) while providing identifiability guarantees is more challenging. This raises the following question: “Can single-snapshot high-resolution DOA estimation be achieved at low computational complexity?”

**Contributions:** This paper answers the above question in the positive by utilizing *sparse sub-arrays* for spatial smoothing. We show that the computational complexity of single-snapshot DOA estimation using subspace methods (implemented on general-purpose solvers) can be significantly reduced—without compromising resolution—by using sparse (rather than ULA) sub-arrays for spatial smoothing. Specifically, given a single-snapshot measurement vector from an  $N$ -antenna ULA, we show that the complexity of subspace methods employing spatial smoothing can be reduced by a factor of  $\sqrt{N}$  using judiciously designed sparse sub-array geometries,

such as nested arrays [13] while provably identifying  $\mathcal{O}(\sqrt{N})$  signal sources/targets. This ‘‘sparse spatial smoothing  $\mathcal{S}^3$ ’’ approach retains a sub-array aperture proportional to that of the full ULA while utilizing all  $N$  measurements. Furthermore, we demonstrate that effective SNR, and thereby resolution, can actually be improved in a desired angular region of interest via a novel shift-domain beamforming method. Simulations validate that sparse array-based spatial smoothing using shift-domain beamforming can offer improved resolution at reduced computational complexity compared to conventional spatial smoothing using ULA sub-arrays.

**Notation:** Given an array geometry  $\mathbb{S} = \{d_1, d_2, \dots, d_M\}$ , matrix  $\mathbf{A}_{\mathbb{S}}(\boldsymbol{\theta}) \in \mathbb{C}^{M \times K}$  denotes the array manifold matrix for sensors located at  $n\lambda/2$ , where  $n \in \mathbb{S}$ ,  $\boldsymbol{\theta} \in [-\pi/2, \pi/2)^K$  denote the target directions, and  $[\mathbf{A}_{\mathbb{S}}(\boldsymbol{\theta})]_{m,n} = \exp(j\pi d_m \sin \theta_n)$ . Furthermore, the aperture of  $\mathbb{S}$  is denoted by  $Aper(\mathbb{S})$ . The largest eigenvalue of  $\mathbf{B}$  is denoted by  $\lambda_{max}(\mathbf{B})$  and  $\mathbf{u}_1(\mathbf{B})$  denotes the eigenvector corresponding to  $\lambda_{max}(\mathbf{B})$ . Moreover,  $vec(\mathbf{V})$  denotes the vectorized matrix  $\mathbf{V}$  and  $w^*$  denotes the conjugate of  $w \in \mathbb{C}$ .

## II. MEASUREMENT MODEL & GENERALIZED SPATIAL SMOOTHING

### A. Measurement Model

Consider  $K$  narrowband source signals impinging on an  $N$ -sensor ULA  $\mathbb{S} = \{0, 1, \dots, N-1\}$  from distinct directions  $\boldsymbol{\theta} = [\theta_1, \theta_2, \dots, \theta_K]^T$ . The single snapshot received signal  $\mathbf{y} \in \mathbb{C}^{N \times 1}$  is of the following form:

$$\mathbf{y} = \mathbf{A}_{\mathbb{S}}(\boldsymbol{\theta})\mathbf{x} + \mathbf{n}, \quad (1)$$

where  $\mathbf{x} \in \mathbb{C}^K$  is the source/target signal and  $\mathbf{n} \in \mathbb{C}^N$  is a noise vector. Note that (1) is applicable to both passive and active sensing—indeed,  $\mathbb{S}$  can represent either a physical or virtual array (i.e.,  $N$  can be the number of physical or virtual sensors). One prominent virtual array model is the sum co-array in active sensing (e.g., co-located MIMO radar [14]). The goal is to estimate  $\{\theta_k\}_{k=1}^K$  from  $\mathbf{y}$ .

### B. Generalized Spatial Smoothing

Spatial smoothing [15] is a widely used technique for single snapshot DOA estimation, where the inherent ‘‘shift invariant’’ structure of certain array geometries—conventionally, ULAs—is leveraged to identify the ‘‘signal subspace’’ of interest from  $\mathbf{y}$ . Specifically, given a so-called basic sub-array  $\mathbb{S}_b = \{d_1, d_2, \dots, d_{N_b}\} \subseteq \mathbb{S}$  and a set of  $Q \in \mathbb{N}_+$  shifted copies of  $\mathbb{S}_b$ , each in  $\mathbb{S}$ , measurement vector  $\mathbf{y}$  is partitioned into vectors  $\mathbf{y}_1, \mathbf{y}_2, \dots, \mathbf{y}_Q \in \mathbb{C}^{N_b}$  corresponding to these shifted sub-arrays  $\mathbb{S}_i = \mathbb{S}_b + \delta_i \subseteq \mathbb{S}$ , where  $\delta_i \in \mathbb{Z}$ ,  $i = 1, 2, \dots, Q$ . These vectors are then rearranged into an augmented measurement matrix:

$$\mathbf{Y} = [\mathbf{y}_1, \mathbf{y}_2, \dots, \mathbf{y}_Q]. \quad (2)$$

In absence of noise ( $\mathbf{n} = \mathbf{0}$ ),  $\mathbf{y}_i$  can be written as  $\mathbf{y}_i = \mathbf{z}_i = \mathbf{A}_{\mathbb{S}_b}(\boldsymbol{\theta})\mathbf{D}_i(\boldsymbol{\theta})\mathbf{x}$ , where  $\mathbf{D}_i(\boldsymbol{\theta}) \in \mathbb{C}^{K \times K}$  is a diagonal matrix

with  $[\mathbf{D}_i(\boldsymbol{\theta})]_{k,k} = \exp(j\pi\delta_i \sin \theta_k)$ . The augmented matrix  $\mathbf{Y}$  therefore permits the following decomposition [16]:

$$\begin{aligned} \mathbf{Y} &= \mathbf{A}_{\mathbb{S}_b}(\boldsymbol{\theta})[\mathbf{D}_1\mathbf{x}, \mathbf{D}_2(\boldsymbol{\theta})\mathbf{x}, \dots, \mathbf{D}_Q(\boldsymbol{\theta})\mathbf{x}] \\ &= \mathbf{A}_{\mathbb{S}_b}(\boldsymbol{\theta})\text{diag}(\mathbf{x})\mathbf{A}_{\Delta}(\boldsymbol{\theta})^T. \end{aligned} \quad (3)$$

where  $\Delta = \{\delta_1, \delta_2, \dots, \delta_Q\}$  represents the set of (integer) shifts.

In conventional ULA-based spatial smoothing,  $\mathbb{S}_b$  and  $\Delta$  are both ULAs with  $N_b$  and  $Q$  satisfying

$$N_b + Q - 1 = N. \quad (4)$$

It is well-known that varying  $N_b$  or  $Q$  for a given  $N$  allows trading off aperture (resolution) for identifiability. A typical choice is  $N_b = \lceil \frac{N}{2} \rceil$ , which maximizes the number of identifiable sources [15].

Eq. (3) illustrates that the shift-invariant structure of  $\mathbb{S}$  enables building the rank of  $\mathbf{Y}$  on which subspace methods can be applied to identify  $\boldsymbol{\theta}$ . In our recent work [16], we investigated generalized spatial smoothing for arbitrary (sparse)  $\mathbb{S}$ ,  $\mathbb{S}_b$  and  $\Delta$  showing when exact recovery is possible. A special case of interest is when  $\mathbb{S}_b$  and  $\Delta$  contain ULA segments. Indeed, it is well-known that the array manifold matrix of an array with a ULA segment of length  $K$  guarantees that the corresponding manifold matrix has a Kruskal rank of at least  $K$  due to containing a Vandermonde sub-array of appropriate size. Therefore, when  $\mathbb{S}_b$  contains a ULA segment of length  $K+1$  and  $\Delta$  contains a ULA segment of length  $K$ , it can be shown that MUSIC can identify  $K$  distinct angles from  $\mathbf{Y}$  [16]. Moreover, note that when  $\mathbb{S}$  is a ULA, as is assumed in this paper, many choices for  $\mathbb{S}_b$  and  $\Delta$  beyond ULAs are possible. Hence, sparse array geometries with a ULA segment of appropriate length (such as nested arrays) can be used for  $\mathbb{S}_b$  in spatial smoothing to increase aperture, and thereby resolution, while guaranteeing the identifiability of a desired number of targets.

### C. Problem Setting

For applying MUSIC, the singular value decomposition (SVD) of  $\mathbf{Y}$  is computed to find the corresponding ‘‘noise subspace’’ with complexity  $\mathcal{O}(\min(N_b^2 Q, N_b Q^2))$  [17]. However, for conventional ULA-based spatial smoothing,  $N_b$  and  $Q$  are usually  $\propto N$ , which will lead to SVD having a complexity of  $\mathcal{O}(N^3)$ . In this paper, we explore spatial smoothing schemes that offer high-resolution DOA estimation at low computational complexity. This may be of great interest in applications such as automotive radar. In particular, we ask:

Q<sub>1</sub> Can we reduce the complexity of SVD by an alternative choice of  $\mathbb{S}_b$  while ensuring: (i) identifiability of  $K$  targets and (ii) an aperture proportional to  $N$ ?

Specifically, we investigate whether sparse arrays, such as nested arrays [13], can answer this question in the positive. Indeed, judicious sparse array designs are known to achieve an aperture on the order of  $N$  using only  $\sqrt{N}$  sensors. By virtue of the ULA segment in the nested array (also with on the order of  $\sqrt{N}$  sensors), identifiability of  $K = \mathcal{O}(\sqrt{N})$  targets via spatial smoothing MUSIC can be guaranteed when shift set

$\Delta$  is a ULA with on the order of at least  $K$  sensors. However, the employed sparse sampling scheme should also use all  $N$  independent measurements in (1), as doing otherwise would be wasteful in presence of noise. Hence, we modify  $\mathbf{Q}_1$  as follows:

$\mathbf{Q}_2$  Can we achieve the goals in  $\mathbf{Q}_1$  while utilizing all  $N$  measurements in (1)—increasing SNR (potentially over a region of interest)—without increasing complexity?

In the next section, we provide a positive answer to this question by showing how to leverage sparse arrays to reduce the computational complexity of subspace methods employing spatial smoothing. We also present a novel shift-domain beamforming approach for spatial smoothing, where multiple sparse spatially smoothed measurement matrices are linearly combined to improve SNR and angular resolution in a given region of interest.

### III. SPARSE SPATIAL SMOOTHING $S^3$ : REDUCED COMPUTATIONAL COMPLEXITY & IMPROVED SNR

To illustrate the main idea of sparse spatial smoothing and shift-domain beamforming, suppose  $\mathbb{S}_b$  is a nested array [13] with  $N_b = 2r(N) - 2 = \mathcal{O}(\sqrt{N})$  sensors, where  $r(N) \triangleq \lfloor \sqrt{N} \rfloor$ . That is,

$$\mathbb{S}_b = \{0, 1, \dots, r(N) - 2\} \cup \{m(r(N) - 1) - 1\}_{m=2}^{r(N)}, \quad (5)$$

with  $Aper(\mathbb{S}_b) = r(N)(r(N) - 1) - 1 = N - \sqrt{N} + C_1 \propto N$  where  $C_1$  is a constant.

The total number of shifts is given by  $N - Aper(\mathbb{S}_b) + 1$ , and we divide them into  $L$  overlapping subsets with each subset of cardinality  $P$  as follows:

$$\begin{aligned} \Delta_1 &= \{0, 1, \dots, P - 1\} \\ \Delta_2 &= \{1, 2, \dots, P\} \\ &\vdots \\ \Delta_L &= \{L - 1, L, \dots, L + P - 2\}. \end{aligned} \quad (6)$$

Note that in this case  $P$  and  $L$  satisfy:

$$L + P = N - Aper(\mathbb{S}_b) + 1, \quad (7)$$

which yields a trade-off between identifiability and complexity. In this paper, we choose  $P = r(N) - C_2 \propto \sqrt{N}$  where  $C_2$  is a constant ( $C_2 \leq 2$  implies the maximum identifiability is  $r(N) - 2$ ). This leads to  $L = \mathcal{O}(1)$ .

The spatially smoothed measurement matrix  $\mathbf{Y}_l$  ( $l = 1, \dots, L$ ) corresponding to  $\mathbb{S}_b$  and  $\Delta_l$  can be represented as (when  $\mathbf{n} = \mathbf{0}$ ):

$$\begin{aligned} \mathbf{Y}_l &= [\mathbf{z}_l, \mathbf{z}_{l+1}, \dots, \mathbf{z}_{l+P-1}] \\ &= \mathbf{A}_{\mathbb{S}_b}(\boldsymbol{\theta}) \text{diag}(\mathbf{x}) \mathbf{A}_{\Delta_l}(\boldsymbol{\theta})^T \\ &= \mathbf{A}_{\mathbb{S}_b}(\boldsymbol{\theta}) \text{diag}(\mathbf{x}) \mathbf{C}_l(\boldsymbol{\theta}) \mathbf{A}_{\Delta_1}(\boldsymbol{\theta})^T, \end{aligned} \quad (8)$$

where the  $p$ -th column of  $\mathbf{Y}_l$  is  $\mathbf{z}_{l+p-1}^{(s)}$ , which contains the elements of  $\mathbf{y}$  corresponding to sub-array  $\mathbb{S}_b + (p + l - 2)$ .  $\mathbf{C}_l(\boldsymbol{\theta}) \in \mathbb{C}^{K \times K}$  is a diagonal matrix with  $[\mathbf{C}_l(\boldsymbol{\theta})]_{k,k} = \exp(j\pi(l-1)\sin\theta_k)$ . Hence, matrix  $\mathbf{C}_l(\boldsymbol{\theta})$  captures the relative shifts between the elements in  $\Delta_l$  and  $\Delta_1$ .

Note that  $\mathbf{Y}_l$  is a  $(2r(N) - 2) \times (r(N) - C_2)$  matrix. Hence  $\mathcal{O}(\sqrt{N})$  targets can be identified by subspace methods applied to  $\mathbf{Y}_l$  due to the ULA segment in  $\mathbb{S}_b$  and  $\Delta_l$ . As we will show later, the complexity of performing SVD on spatially smoothed matrix  $\mathbf{Y}_l$  (corresponding to a nested sub-array) is  $\mathcal{O}(N^{\frac{3}{2}})$ , which is significantly smaller than the complexity  $\mathcal{O}(N^2)$  of performing conventional ULA-based spatial smoothing on a ULA sub-array of equivalent aperture.

For appropriate choice of  $P$ , we can naturally utilize all  $N$  measurements with  $L = 1$ . However, are there any benefits of choosing  $L > 1$  in the presence of noise? Next, we show that the answer is yes: we can improve the effective SNR in a given angular region of interest by taking a suitable weighted sum of  $\{\mathbf{Y}_l\}_{l=1}^L$ . This corresponds to a novel form of beamforming which we denote as “shift-domain” beamforming.

#### A. Shift-domain beamforming

Given complex-valued weights  $\{w_l\}_{l=1}^L \subset \mathbb{C}$ , define the weighted linear combination of all  $\mathbf{Y}_l$  as  $\bar{\mathbf{Y}} := \sum_{l=1}^L \mathbf{Y}_l \cdot w_l^*$ . Hence, by (8),  $\bar{\mathbf{Y}}$  can be rewritten as follows (when  $\mathbf{n} = \mathbf{0}$ ):

$$\begin{aligned} \bar{\mathbf{Y}} &= \sum_{l=1}^L \mathbf{A}_{\mathbb{S}_b}(\boldsymbol{\theta}) \text{diag}(\mathbf{x}) \mathbf{C}_l(\boldsymbol{\theta}) \mathbf{A}_{\Delta_1}(\boldsymbol{\theta})^T \cdot w_l^* \\ &= \mathbf{A}_{\mathbb{S}_b}(\boldsymbol{\theta}) \text{diag}(\mathbf{x}) \underbrace{\left( \sum_{l=1}^L \mathbf{C}_l(\boldsymbol{\theta}) \cdot w_l^* \right)}_{\triangleq \bar{\mathbf{C}}(\boldsymbol{\theta})} \mathbf{A}_{\Delta_1}(\boldsymbol{\theta})^T. \end{aligned} \quad (9)$$

Here,  $\bar{\mathbf{C}}(\boldsymbol{\theta})$  is a  $K \times K$  diagonal matrix

$$\bar{\mathbf{C}}(\boldsymbol{\theta}) = \begin{bmatrix} B(\theta_1) & 0 & \dots & 0 \\ 0 & B(\theta_2) & \dots & 0 \\ \vdots & \vdots & \vdots & \vdots \\ 0 & 0 & \dots & B(\theta_K) \end{bmatrix},$$

where  $B(\theta_k) = \sum_{l=1}^L w_l^* e^{j\pi(l-1)\sin\theta_k}$  denotes the *beam gain* in direction  $\theta_k$ .

#### B. Reduction in Computational Complexity

Next we discuss the computational complexity of the proposed sparse spatial smoothing (“ $S^3$ ”) approach and conventional spatial smoothing approaches using ULA sub-arrays of various sizes. For simplicity, we consider general-purpose solvers applied to the spatially smoothed matrices  $\bar{\mathbf{Y}}$  in (9) and  $\mathbf{Y}$  in (2). Specialized solvers utilizing the structure of said matrices to reduce complexity is left for future work.

Consider  $S^3$  with the nested sub-array  $\mathbb{S}_b$  as in (5) with  $N_b = \mathcal{O}(\sqrt{N})$ ,  $P = \mathcal{O}(\sqrt{N})$ , and  $L = \mathcal{O}(1)$ . Constructing the corresponding spatially smoothed measurement matrix  $\bar{\mathbf{Y}} \in \mathbb{C}^{N_b \times P}$  in (9) requires  $LN_bP$  multiplications / additions (floating point operations), which corresponds to a complexity of  $\mathcal{O}(N)$ . Since the dimensions of  $\bar{\mathbf{Y}}$  are on the order of  $\mathcal{O}(\sqrt{N}) \times \mathcal{O}(\sqrt{N})$ , the dominant computational cost of subspace methods (using general-purpose solvers) is computing the SVD of  $\bar{\mathbf{Y}}$ , which incurs complexity  $\mathcal{O}(N_b P^2) = \mathcal{O}(N^{\frac{3}{2}})$ .

In case of ULA-based spatial smoothing, the basic sub-array  $\tilde{\mathbb{S}}_b$  is a  $\tilde{N}_b$  sensor ULA. We consider three choices of  $\tilde{N}_b$ : the (i) conventional identifiability-maximizing choice,

$\tilde{N}_b = N/2 + 1$  (assuming  $N$  is even for simplicity); (ii) same sub-array aperture as  $S^3$ , i.e.,  $\tilde{N}_b = \text{Aper}(\mathbb{S}_b) = \mathcal{O}(N)$  and; (iii) same number of sub-array sensors as  $S^3$ , i.e.,  $\tilde{N}_b = N_b = \mathcal{O}(\sqrt{N})$ . By (4), the corresponding number of sub-array shifts  $Q$  is (i)  $Q = N/2$ , (ii)  $Q = N - \text{Aper}(\mathbb{S}_b) + 1 = \mathcal{O}(\sqrt{N})$ , and (iii)  $Q = N - N_b + 1 = \mathcal{O}(N)$ . The dimensions of the spatially smoothed matrix  $\mathbf{Y} \in \mathbb{C}^{\tilde{N}_b \times Q}$  are then on the order of (i)  $\mathcal{O}(N) \times \mathcal{O}(N)$ , (ii)  $\mathcal{O}(N) \times \mathcal{O}(\sqrt{N})$ , and (iii)  $\mathcal{O}(\sqrt{N}) \times \mathcal{O}(N)$ . Hence, computing the SVD of  $\mathbf{Y}$  using a general-purpose solver incurs complexity (i)  $\mathcal{O}(N^3)$ , (ii)  $\mathcal{O}(N^2)$ , and (iii)  $\mathcal{O}(N^2)$ .

The above discussion shows that the computational complexity of subspace methods employing spatial smoothing (and general-purpose solvers) can be reduced by a factor of  $\sqrt{N}$  or more using  $S^3$  instead of conventional ULA sub-array based approaches. Section IV will demonstrate this reduction in computational complexity via numerical simulations.

### C. Design of shift-domain beamforming weights to boost SNR over angular region of interest

In presence of noise, shift-domain beamforming also affects the corresponding noise matrix. In this case, each  $\mathbf{Y}_l$  contains an additional spatially smoothed noise matrix  $\mathbf{N}_l \in \mathbb{C}^{N_b \times P}$  (similarly,  $p$ -th column of  $\mathbf{N}_l$  contains the elements of  $\mathbf{n}$  corresponding to sub-array  $\mathbb{S}_b + (p+l-2)$ ). Therefore we have:

$$\begin{aligned} \bar{\mathbf{Y}} &= \mathbf{A}_{\mathbb{S}_b}(\boldsymbol{\theta}) \text{diag}(\mathbf{x}) \bar{\mathbf{C}}(\boldsymbol{\theta}) \mathbf{A}_{\Delta_1}(\boldsymbol{\theta})^T + \sum_{l=1}^L \mathbf{N}_l \cdot \mathbf{w}_l^* \\ &= \mathbf{A}_{\mathbb{S}_b}(\boldsymbol{\theta}) \text{diag}(\mathbf{x}) \bar{\mathbf{C}}(\boldsymbol{\theta}) \mathbf{A}_{\Delta_1}(\boldsymbol{\theta})^T + \bar{\mathbf{N}}(\mathbf{w}) \end{aligned} \quad (10)$$

where  $\mathbf{w} = [w_1, w_2, \dots, w_L]^T \in \mathbb{C}^{L \times 1}$  the shift-domain beamforming weight vector. The question then naturally emerges how to select shift-domain beamforming weights  $\{w_l\}_{l=1}^L$ ? In the following, we optimize these weights to maximize SNR over an angular region of interest. Denote  $\mathbf{a}(\theta) = [1, e^{j\pi \sin \theta}, \dots, e^{j\pi(L-1) \sin \theta}]^T$ , such that  $B(\theta) = \mathbf{w}^H \mathbf{a}(\theta)$ . The effective SNR for a single target with (deterministic) amplitude  $x$  and DOA  $\theta$  is then defined as follows:

$$\text{SNR}(\theta) = \frac{\|x \mathbf{a}_{\mathbb{S}_b}(\theta) \mathbf{w}^H \mathbf{a}(\theta) \mathbf{a}_{\Delta_1}^T(\theta)\|_F^2}{\mathbb{E}(\|\bar{\mathbf{N}}(\mathbf{w})\|_F^2)}. \quad (11)$$

Suppose we have prior knowledge of an angular region of interest  $\Theta = (\theta_l, \theta_h)$  containing the unknown DOAs  $\{\theta_k\}_{k=1}^K$  ( $\theta_l < \theta_k < \theta_h \forall k$ ). This leads to an interesting question: in presence of noise, given a field of view  $(\theta_l, \theta_h)$ , how to design  $\mathbf{w}$  so that the average SNR over  $(\theta_l, \theta_h)$  is maximized? For simplicity, consider the reduced angle  $u = \pi \sin \theta$  and the corresponding region of interest  $\mathbf{U} = (u_l, u_h) = (\pi \sin \theta_l, \pi \sin \theta_h)$ . The optimization problem can be formulated as below:

$$\mathbf{w}_o = \arg \max_{\mathbf{w} \in \mathbb{C}^L} \int_{\mathbf{U}} \text{SNR}(u) du. \quad (12)$$

As Proposition 1 will show, (12) leads to a generalized eigenvalue problem. Surprisingly, this reduces to a Rayleigh quotient maximization problem since the shift between  $\Delta_{l_1}$  and  $\Delta_{l_2}$  ( $l_1 \neq l_2$ ) renders the corresponding noise vectors independent.

**Proposition 1.** Suppose  $\mathbf{n} = [n_1, n_2, \dots, n_N]^T$  where all entries are independent and identically distributed with zero mean and variance  $\sigma^2$ . The solution to (12) is the largest eigenvector of matrix  $\mathbf{A} \in \mathbb{C}^{L \times L}$ ,  $\mathbf{w}_o = \mathbf{u}_1(\mathbf{A})$ , where

$$[\mathbf{A}]_{m,m'} = \begin{cases} \frac{1}{(m-m')j} (e^{j(m-m')u_h} - e^{j(m-m')u_l}) & m \neq m' \\ u_h - u_l & m = m' \end{cases}$$

*Proof.* Note that  $\mathbf{w}^H \mathbf{a}(u)$  is a scalar,  $\|\mathbf{a}_{\mathbb{S}_b}(u) \mathbf{a}_{\Delta_1}^T(u)\|_F^2$  is a constant due to all entries in vectors  $\mathbf{a}_{\mathbb{S}_b}(u)$  and  $\mathbf{a}_{\Delta_1}(u)$  having constant-modulus, and  $x$  is deterministic. Hence,  $\max_{\mathbf{w} \in \mathbb{C}^L} \text{SNR}(u) = \max_{\mathbf{w} \in \mathbb{C}^L} \frac{|\mathbf{w}^H \mathbf{a}(u)|^2}{\mathbb{E}(\|\bar{\mathbf{N}}(\mathbf{w})\|_F^2)}$ . Then we can write

$$\begin{aligned} \mathbf{w}_o &= \arg \max_{\mathbf{w} \in \mathbb{C}^L} \int_{\mathbf{U}} \frac{|\mathbf{w}^H \mathbf{a}(u)|^2}{\mathbb{E}(\|\bar{\mathbf{N}}(\mathbf{w})\|_F^2)} du \\ &= \arg \max_{\mathbf{w} \in \mathbb{C}^L} \frac{\mathbf{w}^H (\int_{\mathbf{U}} \mathbf{a}(u) \mathbf{a}^H(u) du) \mathbf{w}}{\mathbb{E}(\|\bar{\mathbf{N}}(\mathbf{w})\|_F^2)}. \end{aligned} \quad (13)$$

Let  $\mathbf{A}(u) = \mathbf{a}(u) \mathbf{a}^H(u)$  and  $\mathbf{A} = \int_{\mathbf{U}} \mathbf{A}(u) du$ . Then

$$\begin{aligned} [\mathbf{A}]_{m,m'} &= \int_{\mathbf{U}} [\mathbf{A}(u)]_{m,m'} du \\ &= \begin{cases} \int_{u_l}^{u_h} e^{j(m-m')u} du & m \neq m' \\ \int_{u_l}^{u_h} 1 du & m = m' \end{cases} \\ &= \begin{cases} \frac{1}{(m-m')j} (e^{j(m-m')\pi \sin \theta_h} - e^{j(m-m')\pi \sin \theta_l}) & m \neq m' \\ \pi \sin \theta_h - \pi \sin \theta_l & m = m' \end{cases} \end{aligned}$$

Let  $\mathbf{v}_i = \text{vec}(\mathbf{N}_i)$ , denote  $\mathbf{V} = [\mathbf{v}_1, \mathbf{v}_2, \dots, \mathbf{v}_L]$ , then we have:

$$\begin{aligned} \mathbb{E}(\|\bar{\mathbf{N}}(\mathbf{w})\|_F^2) &= \mathbb{E}(\|\sum_{i=1}^L \mathbf{N}_i^{(s)} \cdot w_i^*\|_F^2) \\ &= \mathbb{E}(\|\mathbf{V} \mathbf{w}^*\|_2^2) \\ &= \mathbf{w}^T \underbrace{\mathbb{E}(\mathbf{V}^H \mathbf{V})}_{\mathbf{P}} \mathbf{w}^*. \end{aligned}$$

We now show that  $\mathbf{P}$  is a scaled identity matrix due to the shift between  $\Delta_i$  and  $\Delta_{i'}$  ( $i \neq i'$ ). Define  $N_s \triangleq N_b P$  and let  $\mathbf{v}_1 = [n_{q_1}, n_{q_2}, \dots, n_{q_{N_s}}]^T \in \mathbb{C}^{N_s}$ . Due to the shift between different  $\Delta_l$  in Eq. (6) we have:

$$\begin{aligned} \mathbf{v}_i &= [n_{q_1+(i-1)}, n_{q_2+(i-1)}, \dots, n_{q_{N_s}+(i-1)}]^T \\ \mathbf{v}_{i'} &= [n_{q_1+(i'-1)}, n_{q_2+(i'-1)}, \dots, n_{q_{N_s}+(i'-1)}]^T \\ \mathbb{E}(\mathbf{v}_i^H \mathbf{v}_{i'}) &= \sum_{r=1}^{N_s} \mathbb{E}(n_{q_r+(i-1)}^* n_{q_r+(i'-1)}). \end{aligned}$$

Note that both  $q_r + (i-1), q_r + (i'-1) \in \{1, 2, \dots, N\}$ , if  $i \neq i'$ , then  $q_r + (i-1) \neq q_r + (i'-1)$  and therefore  $n_{q_r+(i-1)}$  is independent of  $n_{q_r+(i'-1)} \forall r \in \{1, 2, \dots, N_s\}$ . Thus,  $\mathbb{E}(\mathbf{v}_i^H \mathbf{v}_{i'}) = 0$  for  $i \neq i'$ .

Using  $\mathbb{E}(\mathbf{v}_i^H \mathbf{v}_j) = 0$  for  $i \neq j$  and  $\mathbb{E}(\mathbf{v}_i^H \mathbf{v}_i) = N_s \sigma^2$ , we have  $\mathbf{P} = N_s \sigma^2 \cdot \mathbf{I}$ . Then Eq. (13) becomes:

$$\begin{aligned} \mathbf{w}_o &= \arg \max_{\mathbf{w} \in \mathbb{C}^L} \frac{\mathbf{w}^H \mathbf{A} \mathbf{w}}{\mathbf{w}^T \mathbf{P} \mathbf{w}^*} \\ &= \arg \max_{\mathbf{w} \in \mathbb{C}^L} \frac{\mathbf{w}^H \mathbf{A} \mathbf{w}}{\mathbf{w}^H \mathbf{w}} \\ &= \arg \max_{\mathbf{w} \in \mathbb{C}^L} R(\mathbf{A}, \mathbf{w}), \end{aligned} \quad (14)$$

where  $R(\mathbf{A}, \mathbf{w})$  is the Rayleigh quotient [18] for  $\mathbf{A}$  and  $\mathbf{w}$ . Since  $R(\mathbf{A}, \mathbf{w}) \leq \lambda_{\max}(\mathbf{A})$ , equality holds if and only if  $\mathbf{w} = \mathbf{u}_1(\mathbf{A})$ .  $\square$

Fig. 1 shows an example beampattern corresponding to the optimal shift-domain weights in (12) for  $\Theta = (10^\circ, 40^\circ)$  and  $L = 11$ . Note that  $\mathbf{w}_o$  can be computed offline once  $\Theta$  is given.

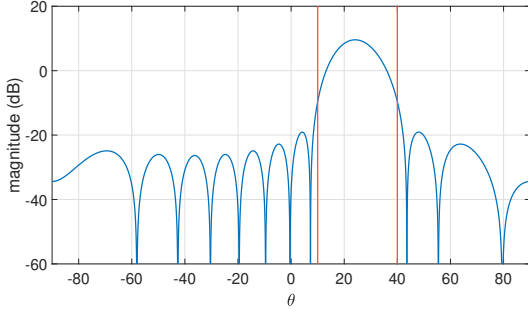


Fig. 1. Beampattern of optimal shift-domain weights in (12). The region of interest in the mainlobe enjoys a beamforming gain (red lines indicate  $\theta_l, \theta_h$ ).

#### IV. SIMULATION RESULTS

In our first simulation, we consider  $K = 3$  sources and  $N = 89$  sensors. The true DOAs are  $\theta = [20^\circ, 25^\circ, 30^\circ]$ , the source/target signals are  $\mathbf{x} = \frac{1+j}{\sqrt{2}}[1, 1, 1]^T$ , and the noise follows a circularly-symmetric complex normal distribution  $\mathbf{n} \sim \mathcal{CN}(0, \sigma^2 \mathbf{I}_{N \times N})$ . We vary noise level  $\sigma$  from 0.1 to 10, which corresponds to an SNR  $\hat{=} 20 \cdot \log_{10} \frac{\min_k(|x_k|)}{\sigma}$ , ranging from 20 dB to -20 dB. We compute the empirical RMSE per source (in degrees) over 200 Monte Carlo trials as  $\text{RMSE} = \sqrt{\frac{1}{200K} \sum_{i=1}^{200} \|\hat{\theta}_i - \theta\|_2^2}$  where  $\hat{\theta}_i = [\hat{\theta}_1^{(i)}, \hat{\theta}_2^{(i)}, \hat{\theta}_3^{(i)}]^T$  is the DOA estimate of the  $i$ -th trial. Spectral MUSIC [6] with a grid size of 20000 is used for DOA estimation.

We compare four spatial smoothing approaches with the following parameter values:

- (i)  $\mathbb{S}_b = \{0, 1, \dots, 7, 15, 23, 31, 39, 47, 55, 63, 71\}$ ,  
 $\Delta_1 = \{0, 1, \dots, 7\}, L = 11$ ;
- (ii)  $\mathbb{S}_b = \{0, 1, \dots, 8, 17, 26, 35, 44, 53, 62, 71, 80\}$ ,  
 $\Delta_1 = \{0, 1, \dots, 8\}, L = 1$ ;
- (iii)  $\mathbb{S}_b = \{0, 1, \dots, 80\}, \Delta_1 = \{0, 1, \dots, 8\}, L = 1$ ;
- (iv)  $\mathbb{S}_b = \{0, 1, \dots, 15\}, \Delta_1 = \{0, 1, \dots, 73\}, L = 1$ .

These cases correspond to (i)  $S^3$  with shift-domain beamforming (nested basic sub-array with  $N_b = 16$  sensors,  $P = 8$  shifts of the basic sub-array per spatially smoothed measurement matrix and  $L = 11$  shift-domain beamforming weights chosen according to Proposition 1 with  $\Theta = (10^\circ, 40^\circ)$ —see Fig. 1); (ii)  $S^3$  without shift-domain beamforming (nested basic sub-array with  $N_b = 17$ ,  $L = 1$  using all  $N$  measurements); (iii) ULA1 with the same basic sub-array aperture as the nested array in (ii); and (iv) ULA2 with the same number of basic sub-array sensors as the nested array in (i).

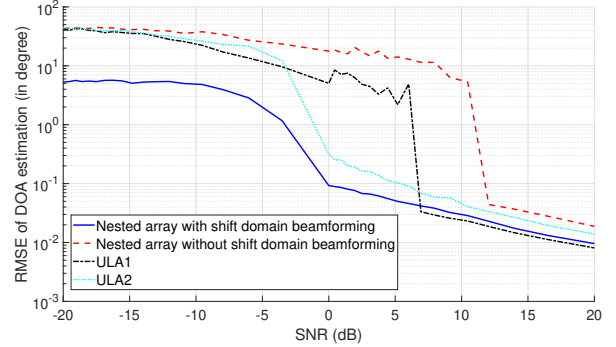


Fig. 2. Average DOA estimation error versus SNR. Sparse spatial smoothing employing shift-domain beamforming (over region  $\Theta = (10^\circ, 40^\circ)$ ) achieves lower error than conventional ULA sub-array-based approaches at low SNR.

Fig. 2 shows the DOA estimation error as a function of SNR. The performance of sparse spatial smoothing  $S^3$  with shift-domain beamforming outperforms conventional ULA-based spatial smoothing when SNR is low, while retaining comparable performance when SNR is high. Fig. 2 also illustrates the fact that resolution is not merely a function of aperture, but also the effective SNR [11] as the improved beamforming gain of  $S^3$  with shift-domain beamforming compensates for its slightly smaller aperture compared to  $S^3$  without shift-domain beamforming. Fig. 3 shows the MUSIC pseudo-spectrum of both  $S^3$  with shift-domain beamforming (top panel) and the two conventional ULA-based spatial smoothing approaches ULA1 (middle panel) and ULA2 (bottom panel) in the case of close DOA separation ( $\theta = [20^\circ, 22^\circ, 24^\circ]$ ). The left column of Fig. 3 shows that when DOA separation is close, ULA2 cannot resolve the DOAs due to its limited aperture. Moreover, when SNR is low (right column of Fig. 3), the beamforming gain of  $S^3$  due to shift-domain beamforming enables resolving all three sources, when both ULA1 (with slightly larger basic sub-array aperture) and ULA2 (with the same number of basic sub-array sensors) fail due to a spurious peak in the MUSIC pseudo-spectrum (likely due to noise shaping by spatial smoothing) and decreased resolution, respectively. Note that  $S^3$  offers this improved performance at a reduced computational complexity, as we demonstrate next.

In our second simulation, we set  $N_b = 2P$  for the nested array  $N = \text{Aper}(\mathbb{S}_b) + L + P - 1$  and vary  $P$  from 5 to 15 (in the previous simulation,  $P = 8$ ). Other parameters remain unchanged. We compare four approaches with the following spatial smoothing parameters:

- (i)  $\mathbb{S}_b = \{0, 1, \dots, P-1, 2P-1, 3P-1, \dots, (P+1)P-1\}$ ,  
 $\Delta_1 = \{0, 1, \dots, P-1\}, L = 11$ ;
- (ii)  $\mathbb{S}_b = \{0, 1, \dots, P-1, 2P-1, 3P-1, \dots, (P+1)P-1\}$ ,  
 $\Delta_1 = \{0, 1, \dots, P+9\}, L = 1$ ;
- (iii)  $\mathbb{S}_b = \{0, 1, \dots, (P+1)P-1\}, \Delta_1 = \{0, 1, \dots, P+9\}, L = 1$ ;
- (iv)  $\mathbb{S}_b = \{0, 1, \dots, 2P-1\}, \Delta_1 = \{0, 1, \dots, P^2+9\}, L = 1$ .

These cases correspond to (i)  $S^3$  with shift-domain beamforming; (ii)  $S^3$  without shift-domain beamforming; (iii) ULA1

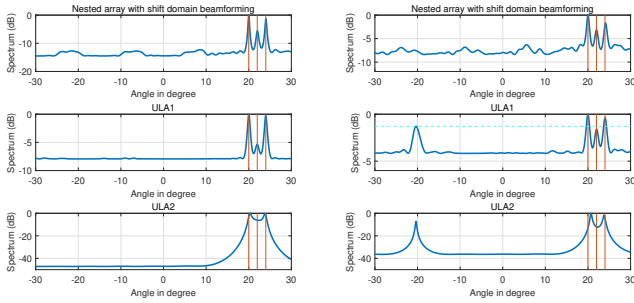


Fig. 3. MUSIC pseudo-spectrum with (left) SNR = 14 dB and (right) SNR = 0 dB.  $S^3$  with shift-domain beamforming (top) provides improved resolution compared to conventional ULA-based spatial smoothing (middle and bottom), especially at low SNR.

with the same basic sub-array aperture as the nested array in (i); and (iv) ULA2 with the same number of basic sub-array sensors as the nested array in (i).

Fig. 4 shows the running time in all four cases—including constructing the spatially smoothed measurement matrix and applying SVD—averaged over 200 Monte Carlo trials. Clearly,  $S^3$  (both with and without shift-domain beamforming) achieves much lower computational complexity than conventional ULA-based spatial smoothing. The size of the corresponding spatially smoothed measurement matrices are (i)  $2P \times P$ ; (ii)  $2P \times (P + 10)$ ; (iii)  $(P^2 + P) \times (P + 10)$ ; and (iv)  $2P \times (P^2 + 10)$ . Note that in absence of prior knowledge of the DOAs, we can still employ  $S^3$  without shift-domain beamforming to achieve high-resolution DOA estimation over the whole angular region at reduced computational complexity.

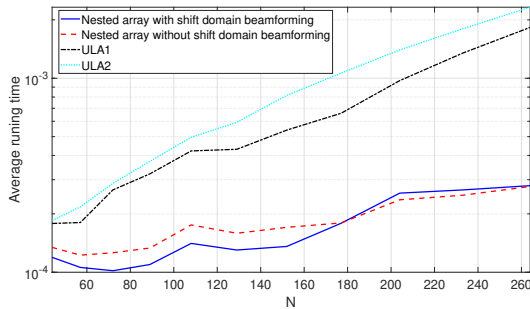


Fig. 4. Average running (elapsed real) time versus number of physical sensors  $N$ . Sparse spatial smoothing achieves significantly lower computational complexity than ULA-based approaches.

## V. CONCLUSIONS

This paper considered the problem of single-snapshot high-resolution DOA estimation. Specifically, we showed that the computational complexity of subspace methods employing spatial smoothing on an  $N$ -antenna ULA can be reduced by a factor of  $\sqrt{N}$  by utilizing suitable sparse (instead of ULA) sub-arrays in the spatial smoothing step. This reduction in complexity is achieved while retaining the aperture and

identifiability of conventional spatial smoothing using ULA sub-arrays when the number of targets is  $\mathcal{O}(\sqrt{N})$ . We also presented a novel beamforming approach to sparse array-based spatial smoothing, where multiple spatially smoothed matrices are linearly combined to improve the effective SNR in a desired angular region. Simulations demonstrated that this so-called shift-domain beamforming method can improve resolution by appropriate beamforming weight design while achieving significantly lower computational complexity than conventional ULA-based spatial smoothing. Future work will explore noise-robust shift-domain beamforming weight designs and sub-array choices for sparse spatial smoothing.

## REFERENCES

- [1] S. M. Patole, M. Torlak, D. Wang, and M. Ali, "Automotive radars: A review of signal processing techniques," *IEEE Signal Processing Magazine*, vol. 34, no. 2, pp. 22–35, 2017.
- [2] J. A. Zhang, F. Liu, C. Masouros, R. W. Heath, Z. Feng, L. Zheng, and A. Petropulu, "An overview of signal processing techniques for joint communication and radar sensing," *IEEE Journal of Selected Topics in Signal Processing*, vol. 15, no. 6, pp. 1295–1315, 2021.
- [3] S. Sun and Y. D. Zhang, "4D automotive radar sensing for autonomous vehicles: A sparsity-oriented approach," *IEEE Journal of Selected Topics in Signal Processing*, vol. 15, no. 4, pp. 879–891, 2021.
- [4] J. Odendaal, E. Barnard, and C. Pistorius, "Two-dimensional super-resolution radar imaging using the MUSIC algorithm," *IEEE Transactions on Antennas and Propagation*, vol. 42, no. 10, pp. 1386–1391, 1994.
- [5] S. U. Pillai and B. H. Kwon, "Forward/backward spatial smoothing techniques for coherent signal identification," *IEEE Transactions on Acoustics, Speech, and Signal Processing*, vol. 37, no. 1, pp. 8–15, 1989.
- [6] R. Schmidt, "Multiple emitter location and signal parameter estimation," *IEEE transactions on antennas and propagation*, vol. 34, no. 3, pp. 276–280, 1986.
- [7] R. Roy and T. Kailath, "ESPRIT-estimation of signal parameters via rotational invariance techniques," *IEEE Transactions on acoustics, speech, and signal processing*, vol. 37, no. 7, pp. 984–995, 1989.
- [8] S. Sun, A. P. Petropulu, and H. V. Poor, "MIMO radar for advanced driver-assistance systems and autonomous driving: Advantages and challenges," *IEEE Signal Processing Magazine*, vol. 37, no. 4, pp. 98–117, 2020.
- [9] I. Roldan, L. Lamberti, F. Fioranelli, and A. Yarovoy, "Low complexity single-snapshot DoA estimation via Bayesian compressive sensing," in *2023 IEEE Radar Conference (RadarConf23)*. IEEE, 2023, pp. 1–6.
- [10] M. Wang and A. Nehorai, "Coarrays, MUSIC, and the Cramér-Rao bound," *IEEE Transactions on Signal Processing*, vol. 65, no. 4, pp. 933–946, Feb 2017.
- [11] P. Sarangi, M. C. Hücümenoğlu, R. Rajamäki, and P. Pal, "Super-resolution with sparse arrays: A non-asymptotic analysis of spatio-temporal trade-offs," *IEEE Transactions on Signal Processing*, pp. 1–14, 2023.
- [12] C.-L. Liu and P. P. Vaidyanathan, "Super nested arrays: Linear sparse arrays with reduced mutual coupling – Part I: Fundamentals," *IEEE Transactions on Signal Processing*, vol. 64, no. 15, pp. 3997–4012, Aug 2016.
- [13] P. Pal and P. P. Vaidyanathan, "Nested arrays: A novel approach to array processing with enhanced degrees of freedom," *IEEE Transactions on Signal Processing*, vol. 58, no. 8, pp. 4167–4181, 2010.
- [14] J. Li and P. Stoica, "MIMO radar with colocated antennas," *IEEE signal processing magazine*, vol. 24, no. 5, pp. 106–114, 2007.
- [15] T.-J. Shan, M. Wax, and T. Kailath, "On spatial smoothing for direction-of-arrival estimation of coherent signals," *IEEE Transactions on Acoustics, Speech, and Signal Processing*, vol. 33, no. 4, pp. 806–811, 1985.
- [16] Y. Bu, R. Rajamäki, P. Sarangi, and P. Pal, "Harnessing holes for spatial smoothing with applications in automotive radar," in *57th Asilomar Conference on Signals, Systems, and Computers*, 2023 (accepted for publication).
- [17] G. H. Golub and C. F. Van Loan, *Matrix computations*. JHU press, 2013.
- [18] R. A. Horn and C. R. Johnson, *Matrix analysis*. Cambridge university press, 2012.